IC/99/202

United Nations Educational Scientific and Cultural Organization
and
International Atomic Energy Agency
THE ABDUS SALAM INTERNATIONAL CENTRE FOR THEORETICAL PHYSICS

# MODELLING OF SEISMIC GROUND MOTION IN SANTIAGO DE CUBA CITY FROM EARTHQUAKES IN ORIENTE FAULT SEISMIC ZONE

Leonardo Alvarez[1]
*Centro Nacional de Investigaciones Sismológicas, Cuba*
*and*
*The Abdus Salam International Centre for Theoretical Physics, SAND Group, Trieste, Italy,*

Giuliano F. Panza
*Department of Earth Sciences, University of Trieste, Trieste, Italy*
*and*
*The Abdus Salam International Centre for Theoretical Physics, SAND Group, Trieste, Italy,*

Franco Vaccari
*Department of Earth Sciences, University of Trieste, Trieste, Italy*
*and*
*Gruppo Nazionale per la Difesa dai Terremoti, 00198 Rome, Italy*

and

Bertha E. González
*Centro Nacional de Investigaciones Sismológicas, Cuba.*

MIRAMARE – TRIESTE
December 1999

[1]Regular Associate of the Abdus Salam ICTP.

**ABSTRACT**

We present the results of complete P-SV and SH waves modelling, up to a maximum frequency of 1 Hz, along two profiles in Santiago de Cuba city. The seismic sources are located, in the depth range from 10 to 40 Km, on the Oriente fault zone, at distances of several tens of kilometres from the city. The calculation has been made by a hybrid method: modal summation in the regional anelastic model (one-dimensional) where the source is buried, and finite differences in the local sedimentary anelastic models (two-dimensional). The analysis of the influence of the depth and of the distance of the source on the site effects shows that standard traditional methods, based on the deconvolution analysis of the rock outcrop motion can lead to erroneous results.

## 1. INTRODUCTION

Santiago de Cuba is the second largest city of Cuba. Located on an active earthquake zone, it experienced the damaging effects of earthquakes since its foundation in the XVI Century, and partial destruction during the earthquakes of 1776 ($M_I \cong 7.6$), 1852 ($M_I \cong 7.2$) and 1932 ($M_s = 6.75$). Furthermore, there exists a high probability of occurrence of an $M_s = 7$ earthquake in the near future (Rubio, 1985), on the Oriente Fault system, located immediately to the South of the city. For this reason several microzoning studies, based mainly on the analysis of engineering-geological conditions, real earthquake effects and microseism registrations have been performed. The first complete microzoning of Santiago de Cuba has been made by González et al. (1989), in the form of maps of expected distribution of seismic intensity and of predominant frequency of shaking, based on microseism' analysis. Recently, by reprocessing all previous results with the aid of a GIS, a map that characterises the expected behaviour of soils has been compiled (Zapata, 1996).

Until present, synthetic seismograms were obtained in two ways: (a) by scaling of weak earthquakes registered on rock (a seismic station located 18 Km from the city) to unconsolidated sediments by considering the transfer functions determined from microseisms (González, 1991); (b) by applying a semi-empirical method developed by Trifunac (1977) which considers only distance, magnitude and soil kind (Zapata, 1996). There are no available seismic records from the city that may be used as a calibration of the computed seismograms.

The methods just mentioned neglect source (focal mechanism and duration) as well as path (regional structure) effects that may have a large influence on the local ground motion. To take into account these effects, we use a method for the calculation of synthetic seismograms in laterally variable anelastic media known as the "hybrid technique" (Fäh, 1992; Fäh et al., 1993, Fäh and Suhadolc, 1994). The main idea is to calculate complete

wave trains generated by a seismic source buried in a regional crust-upper mantle structure, the bedrock structure, and to apply this motion as input to the local structure. The problem is solved in two steps: (a) the P-SV and SH waves signals are generated in the bedrock anelastic structure by the modal summation approach (Panza, 1985; Florsch et al., 1991); (b) these wave trains are used as input, for a finite difference scheme that is used to obtain the waveforms along the local, laterally varying anelastic structure (Fäh, 1992; Fäh et al., 1993).

## 2.GEOLOGICAL SETTING

The territory of the city of Santiago de Cuba and its surroundings covers an area of about 250 $Km^2$ and it is characterised, from the geological point of view, by rocks and unconsolidated sediments of different age, origin and lithological composition.

The oldest rocks that outcrop in the studied territory belong to the "El Cobre" formation, composed mainly by volcano-clastic rocks (various kinds of tuffs, tuffites and agglomerates) of basic and intermediate composition, with intrusions of diorites and granodiorites. The thickness of this formation exceeds 1000 m. The "La Cruz" formation overlays, in a discordant way, El Cobre formation, and it is mainly composed by calcareous conglomerates and sandstones in its lower part, and by organic limestones, in its uppermost part. When the limestones outcrop, they appear intensively meteorised (calcareous eluvium). The thickness of this formation is about 100 m.

The "Santiago" formation is represented by unconsolidated clays and sandy clays with a thickness ranging from 10 to 50 m. The formation outcrops in the north-eastern part of the territory, where a considerable part of the urbanised area is located.

The Quaternary sediment formations are of two kinds. The first one is mainly composed by alluvial and prolluvial soils

(gravels, sands and clays). We can find these soils mostly filling river basins, such as the San Juan River basin, in the eastern part of the city, and their thickness is about 20-30 m. The other kind of Quaternary sediments can be identified bounding the Santiago de Cuba and Cabañas bays, and is composed by sandy clays and peat, as well as man made ground and bay mud. The thickness of this formation is about 10 m.

The Maya formation is composed in its lower part by calcareous conglomerates and gravelites and by hard and dense organic cavern limestones in its upper part. The thickness of this formation ranges from 30 to 50 m. Organic limestones with a wide development of surface karstic phenomena compose the "Jaimanitas" formation. Its thickness ranges between 2 and 20 m. These two formations are very well represented along the seacoasts of the studied territory.

**3.REGIONAL STRUCTURAL MODEL**

The bedrock regional structural model has been compiled from different sources. The uppermost 150 Km are a slight modification of the P and S - wave velocity model routinely used for hypocenter's determination in eastern Cuba (MINBAS, 1989), the density values have been adapted from those proposed by Orihuela and Cuevas (1993), and for all the layers $Q_\alpha = 400$ and $Q_\beta = 200$ (Fig. 1) have been assumed. The upper frequency limit for the numerical simulation has been fixed in 1 Hz, because the available structural model is not detailed enough to warrant computations reliable at higher frequencies. Our results can be directly applied to ten and more storey buildings, lifelines, etc. This possibility is very important for Santiago de Cuba city, where approximately 10 years ago a program of construction of typical 12, 15 and 18-storey buildings began, and measurements of microseisms show that free oscillation periods of 18-storey buildings are in the range 0.8-1.2 seconds (González, 1998; Seo et al., 1998).

## 4.TWO DIMENSIONAL STRUCTURAL PROFILES IN THE CITY

To study the influence of local soil conditions on seismic input, we select two profiles in different parts of the city, that cross the main structural formations (with exclusion of the coastal Maya and Jaimanitas ones). Profile A, with a length of 12 Km, goes along the San Juan River Basin, while profile B, 10 Km long, crosses the northern part of Santiago de Cuba bay, through the industrial part of the city and some urbanised areas. The two profiles are located at about 40 Km and 80 Km from the sources A and B, respectively. The two sources belong to the Oriente transform fault system, where the expected strong earthquakes are likely to be located (Fig. 2).

For both profiles, a 200 m deep cross section has been constructed, considering the characteristic soils of Santiago de Cuba (González et al., 1989) and with the aid of geotechnical boreholes data. The mechanical properties of the materials (P- and S-wave velocities and quality factors) have been selected from specialised literature (Pavlov 1984; Japan Working Group for TC-4 Committee, 1992) and in some cases are supported by laboratory measurements.

## 5. P-SV AND SH-WAVES SEISMIC INPUT MODELING

The hybrid approach developed by Fäh (1992) is used to model the seismic input in the investigated area. Wave propagation from the source up to the 2D local structure is computed with the modal summation technique (Panza, 1985; Florsch et al., 1991), using the layered bedrock structure, representative of the path from the source to Santiago de Cuba, while finite differences are used to model the wavefield along the profiles selected in the city. The effectiveness of the boundary conditions applied to the model treated with the FD scheme is tested by computing, with the FD technique, the signals corresponding to the regional bedrock structure at selected sites along the profile, and comparing such results with the signals obtained with modal summation (for more details see Fäh, 1992).

The sites along both profiles are placed at intervals of 900 m. For each site we calculate displacement, velocity and acceleration seismograms for a point source with seismic moment $Mo = 1.0 \times 10^{13}$ N-m, focal depth h = 30 Km, and focal mechanism: dip = 21º, azimuth = 302º and rake = 21º. This mechanism corresponds to the Harvard University determination of one local earthquake that can be considered representative of sources A and B. These seismograms have been then scaled for a possible earthquake of Ms = 7.0 ($Mo = 3.55 \times 10^{19}$ N-m) by using the scaling law of Gusev (1983), as reported by Aki (1987).

**6.RESULTS**

The lateral variations present in the local structures produce great variations in the seismograms. As it could be expected, there is an increment of the signal duration and of the maximum amplitudes with respect to the bedrock signals, and in some cases the wave shape changes drastically (Fig. 3). Examples of velocity seismograms scaled for a Ms=7 earthquake are shown in Fig. 4. The maxima and minima of the peak values of ground motion and design ground acceleration (DGA) obtained by scaling acceleration seismograms with the design response spectra for rock sites of Cuban building code (Norma Cubana, 1999), along both profiles, are given in Table 1. As a comparison, macroseismic intensities equivalent to displacement values have been determined from the relationships obtained by Panza et al. (1997) and Alvarez et al. (1999) and are presented in Table 2.

In the frequency domain, in general, a sharp increase of the amplitudes in the range 0.75-1.0 Hz is observed and at these frequencies the acceleration spectra are strongly dependent on the site, as can be seen from Fig. 5.

Useful estimation of the local effects can be made by computing the response spectra ratio (RSR). For each site where we have made the computations we look at the transfer function defined by the ratio **RSR = [RS(2D)]/[RS(1D)],** where RS(2D) is the response spectrum (at 5% of damping) of the signal

calculated for the laterally varying structure, and RS(1D) is the one calculated for the bedrock structure. In Fig. 6 we show the RSR for the three components of motion, along the two profiles.

## 7.DISCUSSION

The RSR of Fig. 6 show the influence of the soft sediments on ground motion. For frequencies below 0.4 Hz the RSR are very low, while large local maxima appear in the range 0.8-1.0 Hz. Along the profiles, the position of these maxima varies with varying components of motion. Along both profiles, the RSR maxima for vertical P-SV and SH waves are localised where there is a large variation of the relative thickness of the first two sedimentary layers, between sites 3 and 8. For the radial P-SV waves, the increment of the RSR in the sites with a strong gradient in the thickness of sediments appears as a local maximum, hidden by the absolute maximum at the end of the profile.

The peak amplitude values along each profile, given in Table 1, show that there is a wide variability, not only from site to site, but also between the different components. Along each profile, in spite of the multiplicity of conversion formulae considered to convert displacements into intensities, the seismic intensity varies only within one degree (Table 2).

### 7.1 Source influence on site effects

Standard microzoning procedures more or less explicitly assume that the spectral ratios are independent from the source depth, distance and focal mechanism. This assumption may be acceptable when the subsurface geometry of the different lithologic units is simple and when single non-interfering seismic waves are considered, but in general represents an approximation too rough to allow to obtain reliable results (Panza et al., 1999a). This limit of standard microzoning procedures is evidenced by recent data that have shown that the recorded motions at the bedrock differ significantly from that obtained

from a deconvolution analysis of the rock outcrop motion (Field, 1996; Riepl et al., 1998).

The effect of the source mechanism has been investigated in some detail by Romanelli and Vaccari (1999) and Panza et al. (1999b). Here we consider the effect of the source position on RSR performing the following tests.

We analyse the influence of the source depth variation in the range from 10 to 40 km along profile B (on average about 85 Km from the source). For depths in the range from 10 to 20 km and below 30 km, the large absolute maximum at about 10 km from the beginning of the profile (sites 10 and 11), clearly visible in Fig. 6d, does not appear, and the absolute maximum is located between sites 2 and 5, in correspondence of the gradient of the thickness of the sediments. Therefore the large maximum is clearly evident only if the source depth varies from 30 km (Fig. 6d) to about 20 Km.

When the same analysis is performed for profile A, that on average is at about 45 km from the source, there are variations in the details of the picture of the RSR, but the main features remain visible, with the exception of the large maximum that now is absent.

Keeping the source at a depth of 30 km, we consider different distances, from the beginning of profile B, in the range from 40 to 120 Km and we observe that the large absolute maximum is present for distances in the range from 60 to 120 Km from source. Similarly we can conclude that for profile A this critical distance varies in the range from 70 to 90 Km.

Another test is made to investigate the profile geometry effects on polarization. We consider simple 1-layer and 2-layer structural models, whose mechanical properties correspond to the different units present in both profiles. Both El Cobre and La Cruz formations, alone or combined, give an RSR picture very close to the one presented in Fig. 6d. The sedimentary formations instead, when alone, produce smaller amplitude maxima at a frequency of 0.5-0.6 Hz distributed along the profile, and when combined with the El Cobre formation they

tend to shift the maximum to lower frequencies and closer to the source.

We can therefore conclude that the large absolute maximum is due to waves critically reflected at the Moho and then polarised by the low velocity sediments, mainly those corresponding to La Cruz and El Cobre formations. Within our geometry such phenomena become relevant for distances in the range from 60 to 120 Km, and for focal depths in the range from about 20 to 30 Km. A similar effect is observed at distances as large as 150 Km, but the small amplitudes of the waves involved (almost four times smaller than those at 80 Km) make this effect irrelevant for our purposes.

The critical reflection effect has been detected in real data by Burger et al. (1987). They found that in North America the pseudo velocity calculated at 1 Hz and 5% of damping does not obey a simple distance-decay law, but in the distance range 60-150 Km remains approximately constant, if not increasing, with increasing distance.

**7.2 Comparison with previous seismic microzoning results**

Our results may be compared with previous seismic microzoning of Santiago de Cuba, made by Gonzalez et al. (1989), Gonzalez (1991) and Zapata (1996). The first two investigations, mainly based on the analysis of the engineering-geological conditions of the city and on the measurements of microseisms (vertical velocity) in the frequency bands centered at 0.31,0.62, 1.28, 2.5, 5, 10 and 27 Hz, supply two different maps, one with intensity variation estimates based on engineering-geological soil conditions and the other showing the predominant frequency of the measured microseisms. Zapata (1996), with the aid of a GIS system, reanalysed all the information contained in the two papers by González et al. (1989) and González (1991) and added the results of microseism measurements (3-component displacement) in the frequency range (0.6 - 6 Hz), as well as other geomorphological and geological data. Zapata (1996) produced a new microzoning map, which divides the study area in 5 categories, and he supplied a somewhat fuzzy correlation with

the expected variations of the macroseismic intensity. In Fig. 7a and 7b we report the map of intensity variations of González et al. (1989) (map G1 in the following) and the microzoning map of Zapata (1996) (map Z in the following), together with the trace of the profiles A and B and the position of the sites where we computed the synthetic seismograms. By simple inspection of the maps it is clear that their characteristic along the profiles are different. In the case of map G1, both profiles begin from a high level of seismic hazard and gradually pass to a low one. This is not the case for map Z. In this map, profile A crosses a zone with a complicated pattern, and it is not possible for some sites to determine the exact category, while profile B crosses a zone with almost constant, low level, seismic hazard.

The peak values of the ground motion show an acceptable agreement in the general trend along both profiles in the case of map G1, while for map Z the agreement is, in general, much worse, even if the differences are within one degree of intensity. The gradients in seismic intensity in G1 and Z maps are larger than the ones derived from synthetic seismograms, probably because of the difference in the cut off frequency of the different data sets: 1 Hz for synthetic signal and 27 Hz for G1 and Z maps. The analysis of this problem will be subject of a future investigation. However, the main difference between G1 and Z maps on one side, and our results on the other, are the effects due to critical reflections. These effects are entirely neglected in G1 and Z maps, because the procedure followed in their compilation does not take into account the propagation trajectory of the waves from the possible sources to the city.

## 8. CONCLUSIONS

Considering as scenario earthquakes two Ms=7 events, representative of a seismogenic zone immediately south of the city, the Oriente fault zone, we study, along two profiles

crossing Santiago de Cuba city, the influence of the regional structure and of the local soil conditions on ground motion.

In the cases of radial P-SV waves generated by a source located in a depth range from 20 to 30 Km, at an epicentral distance ranging from 60 to 120 Km, we observe, in the frequency interval 0.8-1 Hz, a strong amplification effect along the profile located North of Santiago de Cuba Bay. For the other profile the same phenomenon is observed in the range of distances from 70 to 90 Km. This effect is due to waves critically reflected at the Moho and then polarised by the low velocity sediments, mainly those corresponding to La Cruz and El Cobre formations.

Where comparable, our results follow the general trend of the previous investigations considered, and the differences between our estimates of intensity variation and those reported in maps G1 and Z, are within one degree of intensity. The effect of the critical reflection evidenced by our analysis cannot be accounted by the procedure followed by González et al. (1989) and Zapata (1996).

**ACKNOWLEDGEMENTS**

This work was partially supported by ICTP grants (TRIL Programme and the Associateship Programme) and from IUGS-UNESCO-IGCP Project 414: "Realistic Modelling of Seismic Input for Megacities and Large Urban Areas".

**REFERENCES**

AKI, K. (1987): Strong motion seismology. In: Erdik, M.Ö and Toksöz, ed. Strong Ground Motion Seismology, NATO ASI Series, Series C: Mathematical and Physical Sciences, vol. 204, pp. 3-41. D. Reidel Publishing Company, Dordrecht.

BURGER, R. W.; SOMERVILLE, P.G.; BARKER, J.S.; HERRMANN, R.B. and HELMBERGER D.V. (1987): The effect of crustal structure on strong ground motion attenuation relations in eastern North America. Bull. Seism. Soc. Am., vol. 77, No. 2, pp. 420-439.

ALVAREZ, L.; VACCARI, F.; PANZA, G.F.(1999): Deterministic seismic zoning of eastern Cuba. Pure and Applied Geoph., vol.156, pp. 469-486.

FÄH, D. (1992): A hybrid technique for the estimation of strong ground motion in sedimentary basins. Ph.D. Thesis, Nr. 9767, Swiss Fed. Inst. Technology, Zurich 161 pp.

FÄH, D.; IODICE, C.; SUHADOLC, P.; PANZA, G.F. (1993): A new method for the realistic estimation of seismic ground motion in megacities, the case of Rome. Earthquake Spectra, vol. 9, No. 4, pp. 643-668.

FÄH, D. and SUHADOLC, P. (1994): Application of numerical wave propagation techniques to study local site effects: The case of Benevento (Italy). Pure and Applied Geoph., vol. 143, pp. 513-536.

FIELD, E. H., (1996): Spectral amplification in a sediment-filled valley exhibiting clear basin-edge-induced waves, Bull. Seism. Soc. of Am., 86, No. 4, pp. 991-1005.

FLORSCH, N. FÄH, D.; SUHADOLC, P.; PANZA, G.F. (1991): Complete synthetic seismograms for high-frequency multimode SH-waves. Pure and Applied Geophys., vol. 136, No. 4, pp. 529-560.

GONZÁLEZ, B.E. (1991): Estimación del efecto sísmico en la ciudad de Santiago de Cuba. Tesis en opción al grado de Candidato a Doctor en Ciencias Físicas. Instituto de Geofísica y Astronomía, La Habana.

GONZÁLEZ, B.E.; MIRZOEV, K.M.; CHUY, T.; GOLUBIATNIKOV, V.L.; LYSKOV, L.M.; ZAPATA, J.A.; ALVAREZ, H. (1989): Microzonación sísmica de la ciudad de Santiago de Cuba. Comunicaciones Científicas sobre Geofísica y Astronomía, No. 15, 25 pp. Instituto de Geofísica y Astronomía, Academia de Ciencias de Cuba.

GONZÁLEZ, B.E.(1998): El método de los microsismos en la solución de tarea de la sismología Ingenieril, Memorias del III Congreso cubano de Geología y Minería (GEOMIN98), vol. I, pp. 284-286. Editorial Palcograf, ISSN 939-7117-01-0.

GUSEV, A.A. (1983): Descriptive statistical model of earthquake source radiation and its application to an estimation of short period strong motion. Geophys. J. R. Astron. Soc. vol. 74, pp. 787-800.

JAPAN WORKING GROUP FOR TC-4 COMMITTEE (1992): Seismic Zoning on Geotechnical Hazards (Draft).

MINBAS (1989): Investigaciones complejas para la ubicación de una central electronuclear en la provincia Holguín. Tomo 1: Trabajos Sismológicos. Libro 9, parte 2: Informe sobre los materiales del procesamiento de la red de estaciones sismológicas. Internal Report, Ministry of Basic Industry, Cuba, 360 pp.

NORMA CUBANA (1999): Propuesta de nueva norma cubana sismorresistente, 110 pp., (Draft).

ORIHUELA, N. and CUEVAS, J. L. (1993): Modelaje sismogravimétrico de perfiles regionales del Caribe central, Revista Ingeniería, Universidad Central de Venezuela, 8, pp. 55-73.

PANZA, G. F. (1985): Synthetic seismograms: the Rayleigh waves modal summation, J. Geophys. Res., 58, pp. 125-145.

PANZA, G. F., CAZZARO, R. and VACCARI, F. (1997): Correlation between macroseismic intensities and seismic ground motion parameters. Annali di Geofisica, vol. XL, No. 5, pp. 1371-1382.

PANZA, G.F.; ROMANELLI, F. and VACCARI, F. (1999a): Seismic waves propagation in laterally heterogeneous elastic media:

Theory and applications to the seismic zonation. Advances in Geophysics, in press.

PANZA, G. F., VACCARI, F., COSTA, G., SUHADOLC, P. and FÄH, D. (1996), Seismic input modelling for zoning and microzoning, Earthquake Spectra, *12*, pp. 529-566.

PANZA, G.F., VACCARI, F. and ROMANELLI, F., (1999b): The IUGS-UNESCO IGCP Project 414: Realistic modeling of Seismic Input for Megacities and Large Urban Areas. Episodes, vol. 22, No 1.

PAVLOV O.Y., red. (1984): Seismic microzoning (in Russian). Moscow, Nauka.

RIEPL, J., BARD, P.-Y., HATZFELD, D., PAPAIOANNOU, C., and NECHTSHEIN, S., (1998): Detailed evaluation of site-response estimation methods across and along the sedimentary valley of Volvi (EURO-SEISTEST), Bull. Seism. Soc. Am., vol. 88, pp. 488-502.

ROMANELLI F. and VACCARI F. (1999): Site response estimation and ground motion spectral scenario in the Catania Area, J. Seism., 3, 311-326.

RUBIO, M. (1985): The assessment of seismic hazard for the Republic of Cuba. Ph.D. Thesis, Institute of Geophysics, Science Academy of Czechoslovakia, Prague.

SEO,K.; GONZALEZ, B.E.; ARANGO, E. et al. (1998): Past, present and perspective research on seismic microzonig in the cities of Santiago de Cuba and Havana. Proceedings of the Workshop to Exchange Research Information in the International Scientific Research Project "Joint Study on Seismic Microzonation in Earthquake Countries", Tokyo Institute of Technology, Japan, 17 pp.

TRIFUNAC, M.D. (1977): Methods for prediction of strong earthquake ground motion. Final Technical Report, October 1, 1976 - September 30, 1977. Prepared for the U.S. Nuclear Regulatory Commision, NUREG-0406, Vol. 1.

ZAPATA, J.A. (1996): Utilización de variantes metodológicas de microzonificación sísmica en la ciudad de Santiago de Cuba.

Tesis en opción al grado de Doctor en Ciencias Geofísicas. Centro Nacional de Investigaciones Sismológicas, Santiago de Cuba.

*Table 1.* Peak values for displacement D (cm), velocity V (cm/sec.) acceleration A (cm/sec$^2$) for a maximum frequency of 1 Hz([1]) and design ground acceleration DGA, along the considered profiles.

a) Maximum

| Comp. of motion | San Juan River (Profile A) | | | | Santiago Bay (Profile B) | | | |
|---|---|---|---|---|---|---|---|---|
| | D | V | A | DGA | D | V | A | DGA |
| radial | 3.52 | 1.62 | 5.75 | 23.2 | 0.91 | 1.65 | 8.49 | 40.2 |
| vert. | 5.95 | 1.53 | 4.69 | 15.6 | 1.32 | 1.63 | 6.63 | 20.4 |
| Trans. | 3.35 | 6.06 | 26.5 | 92.0 | 1.07 | 1.48 | 6.16 | 22.8 |

b) Minimum

| Comp. Of motion | San Juan River (Profile A) | | | | Santiago Bay (Profile B) | | | |
|---|---|---|---|---|---|---|---|---|
| | D | V | A | DGA | D | V | A | DGA |
| Radial | 3.00 | 0.85 | 2.85 | 10.8 | 0.75 | 0.95 | 4.56 | 21.5 |
| Vert. | 1.13 | 1.27 | 2.64 | 7.0 | 0.78 | 1.21 | 4.70 | 15.0 |
| Trans. | 2.14 | 2.64 | 11.6 | 41.7 | 0.81 | 0.90 | 3.27 | 10.5 |

([1]) It is well known that the acceleration at 1 Hz is not representative of the absolute maximum, that for this parameter of ground motion in general occurs at higher frequencies (e.g. Panza et al., 1997). Nevertheless it can be extrapolated to high frequencies by using the design response spectra, commonly included in seismic building codes (a rough estimation of peak ground acceleration can be obtained from maximum spectral value - MSV, through MSV=2.5*DGA); a discussion of this procedure can be found in Panza et al.(1996) and Alvarez et al. (1999).

*Table 2.* Macroseismic intensities (MSK) converted from D values of Table 1 by using linear relationships of Panza et al. (1997) (1, 2) and Alvarez et al. (1999) (3, 4). The values corresponding to each component and to the maximum of all components are given.

a) Maximum

| Comp. of motion | San Juan River (Profile A) | | | | Santiago Bay (Profile B) | | | |
|---|---|---|---|---|---|---|---|---|
| | 1 | 2 | 3 | 4 | 1 | 2 | 3 | 4 |
| radial | IX | VIII | VIII | VII | VI | VII | VI | V |
| vert. | IX | VIII | IX | VIII | VII | VII | VII | VI |
| trans. | VIII | IX | VIII | VII | VII | VI | VI | V |
| max. | IX | IX | IX | VIII | VII | VII | VII | VI |

b) Minimum

| Comp. of motion | San Juan River (Profile A) | | | | Santiago Bay (Profile B) | | | |
|---|---|---|---|---|---|---|---|---|
| | 1 | 2 | 3 | 4 | 1 | 2 | 3 | 4 |
| radial | VIII | VIII | VIII | VII | VI | V | VI | V |
| vert. | VII | VI | VI | VI | VI | V | VI | V |
| trans. | VIII | VII | VI | VI | VI | V | VI | V |
| max. | VIII | VIII | VIII | VII | VI | V | VI | V |

**FIGURE CAPTIONS**

*Fig. 1.* Regional bedrock structural model used in the calculations. a) Details of the first 200 Km, b) Whole depth range.

*Fig. 2.* a) Geographical location of the study region, b) Position of the profiles and of the sources considered.

*Fig. 3.* Comparison of velocity seismograms calculated for a $Mo=1.0x10^{13}$ N-m earthquake for points in the middle of both profiles with the ones calculated at equivalent distances in bedrock regional structure. Profile A: (a) - radial, (b) - vertical and (c) - transverse. Profile B: (d) - radial, (e) - vertical and (f) - transverse. All components are normalised to the absolute maximum ($6.29x10^{-3}$ cm/sec.) of the set.

*Fig. 4.* Expected ground motion velocities normalised to maximum absolute peak amplitude (see table 2) along the profile from an Ms=7 earthquake. (a) - profile A, San Juan River; (b) - profile B, Santiago Bay. Cross-sections and mechanical properties for each layer are also shown.

*Fig. 5.* Acceleration amplitude spectra for the synthetic signals for a $Mo=1.0x10^{13}$ N-m earthquake in the considered sites along both profiles. (a),(b) and (c) - profile A; (d), (e) and (f) profile B.

*Fig. 6.* Relative response spectra as a function of frequency along each profile. (a), (b) and (c) - profile A; (d), (e)and (f) - profile B.

*Fig. 7.* Seismic microzoning maps of Santiago de Cuba: a) Modified from Gonzalez et al. (1989), as a function of intensity increments [1 - $\Delta I \geq 1$, 2 - $\Delta I = 1$, 3 - $\Delta I = 0$, 4 - $\Delta I = -1$] b) Modified from Zapata (1996) [1 - very favourable, 2 - favourable, 3 - middle, 4 - unfavourable, 5 - very unfavourable]. With respect to intensity, the classification of Zapata (1996) is { (1,2) - $\Delta I = (-0.5, -1)$, 3 - $\Delta I = (0, 1)$, (4,5) - $\Delta I =$ (1, 2 or more)}. Profiles and sites, ordered from SW to NW, of our computations are indicated with solid lines and full circles respectively.

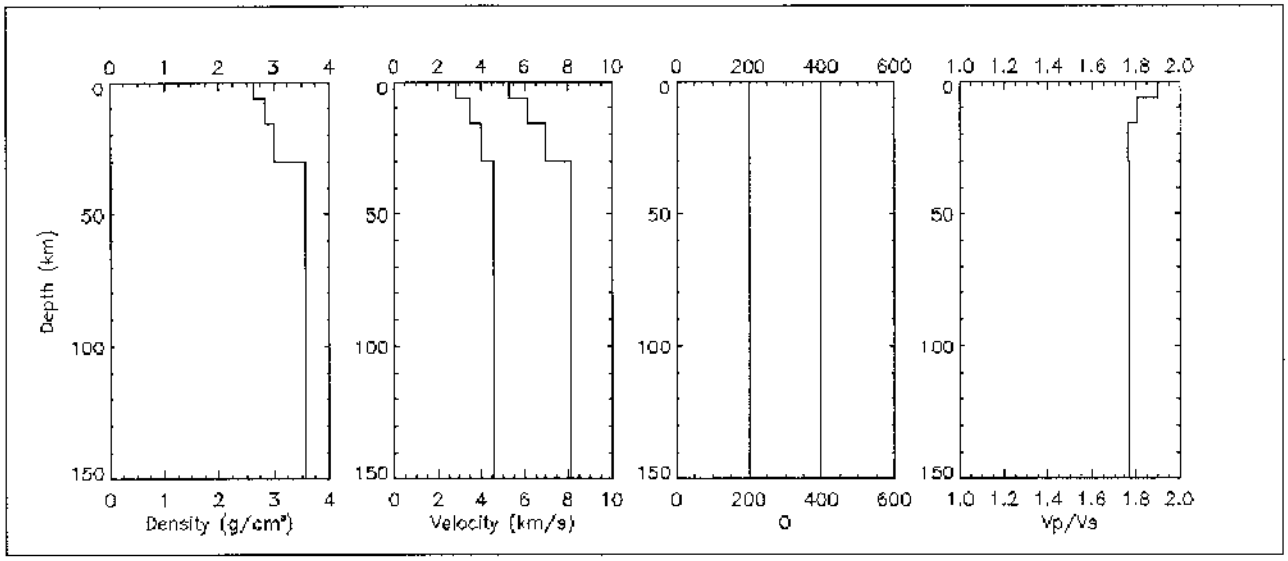
Depth (km)
Density (g/cm³)
Velocity (km/s)
Q
Vp/Vs

a)

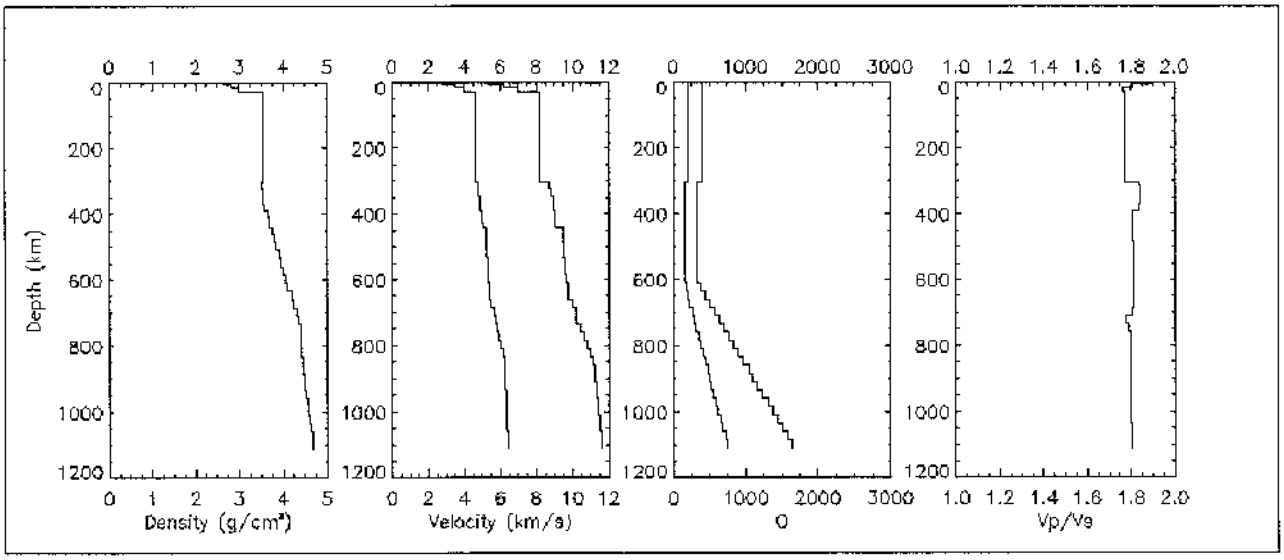
Depth (km)
Density (g/cm³)
Velocity (km/s)
Q
Vp/Vs

b)

Fig. 1

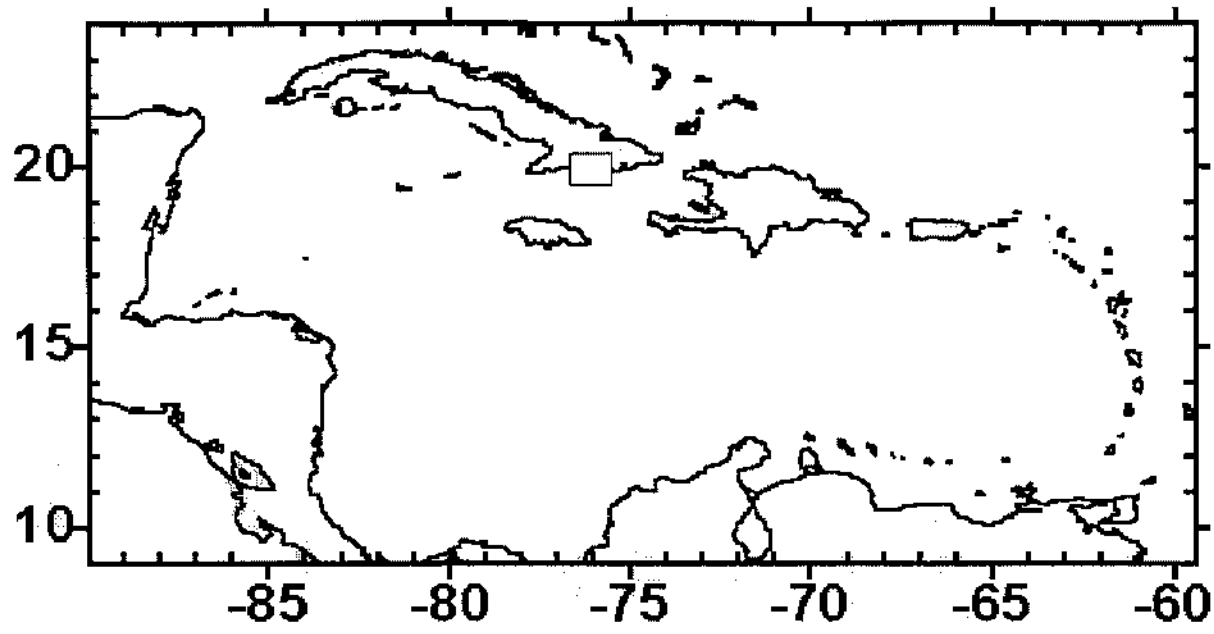
20
15
10
-85
-80
-75
-70
-65
-60

(a)

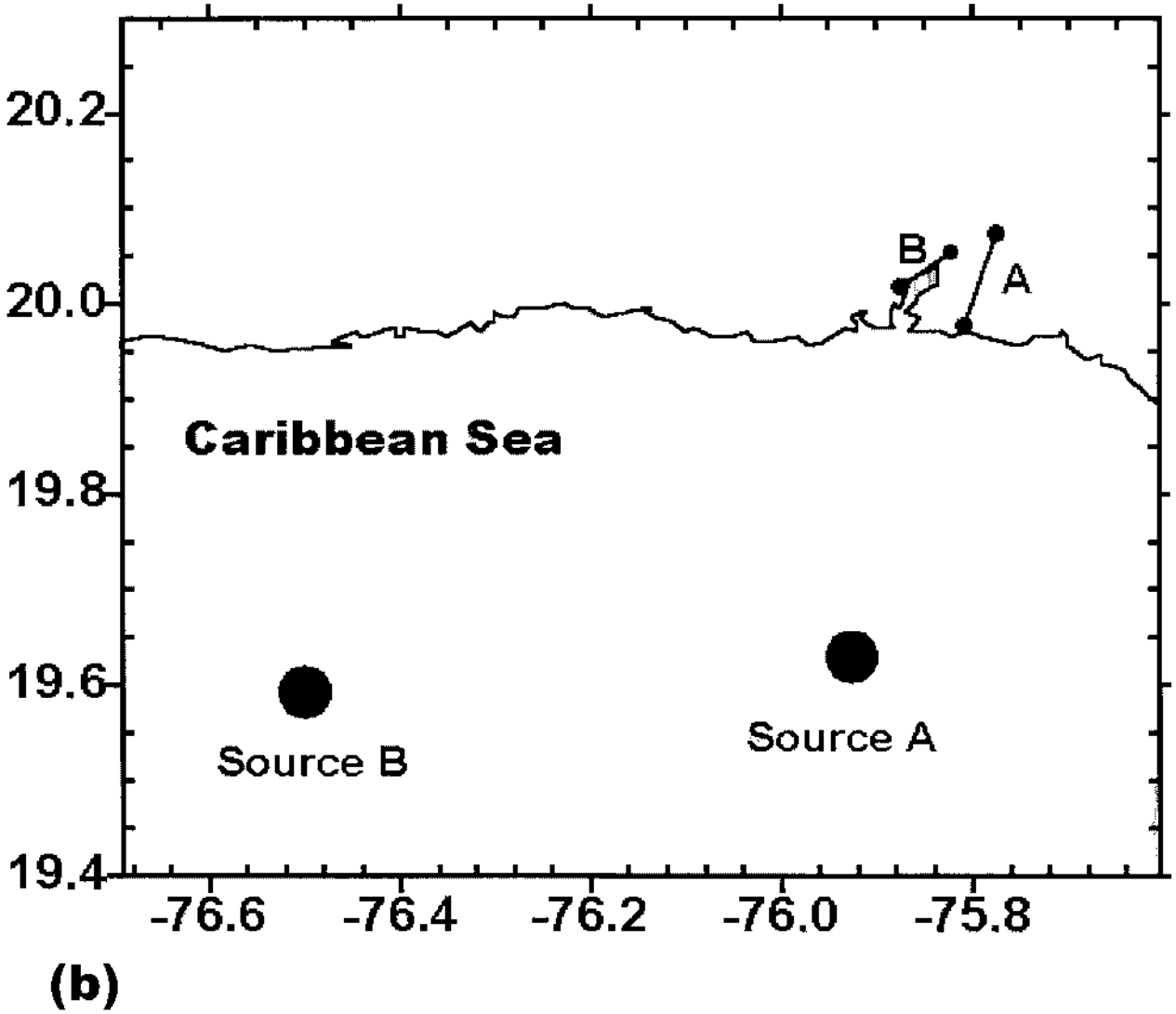
20.2
20.0
19.8
19.6
19.4
B
A
Caribbean Sea
Source B
Source A
-76.6
-76.4
-76.2
-76.0
-75.8

(b)

Fig. 2

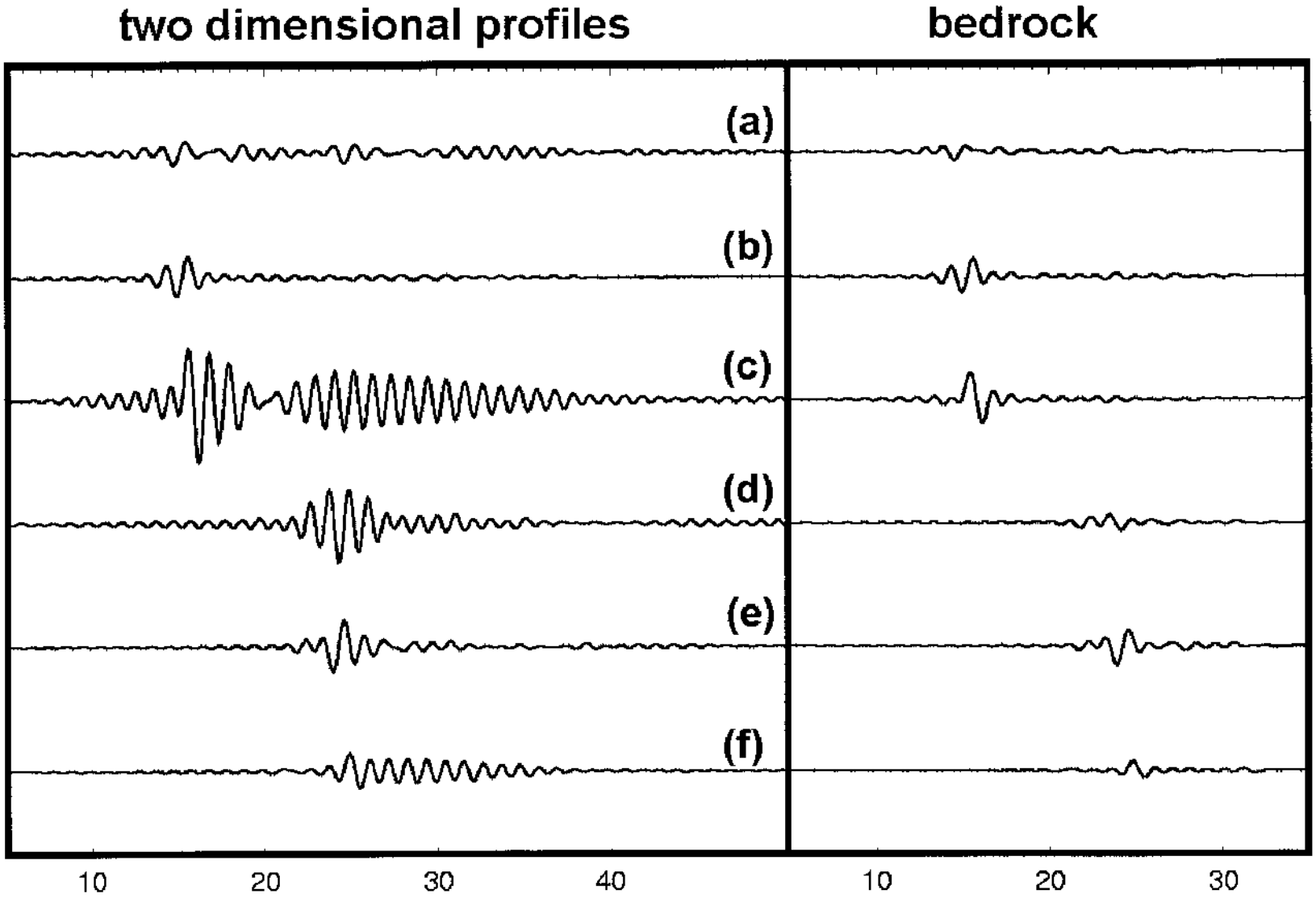


Fig. 3

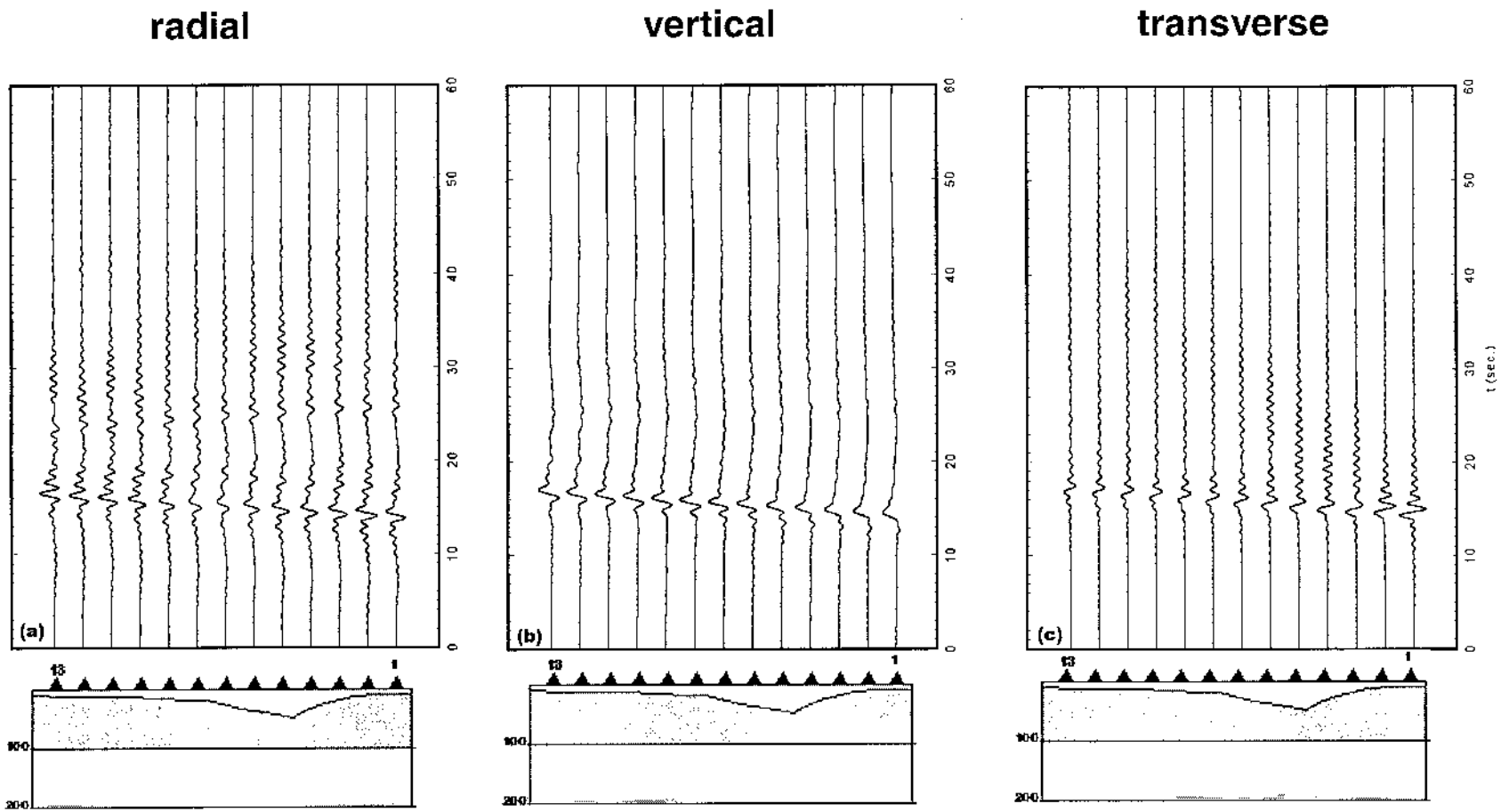


| No | Density | Vp | Vs | Qp | Qs |
|---|---|---|---|---|---|
| 1 | 1.8 | 1.7 | 0.4 | 100 | 50 |
| 2 | 2 | 1.9 | 0.6 | 200 | 100 |
| 3 | 2.3 | 2.2 | 0.8 | 400 | 200 |

1
2
3

Fig. 4 (a-c)

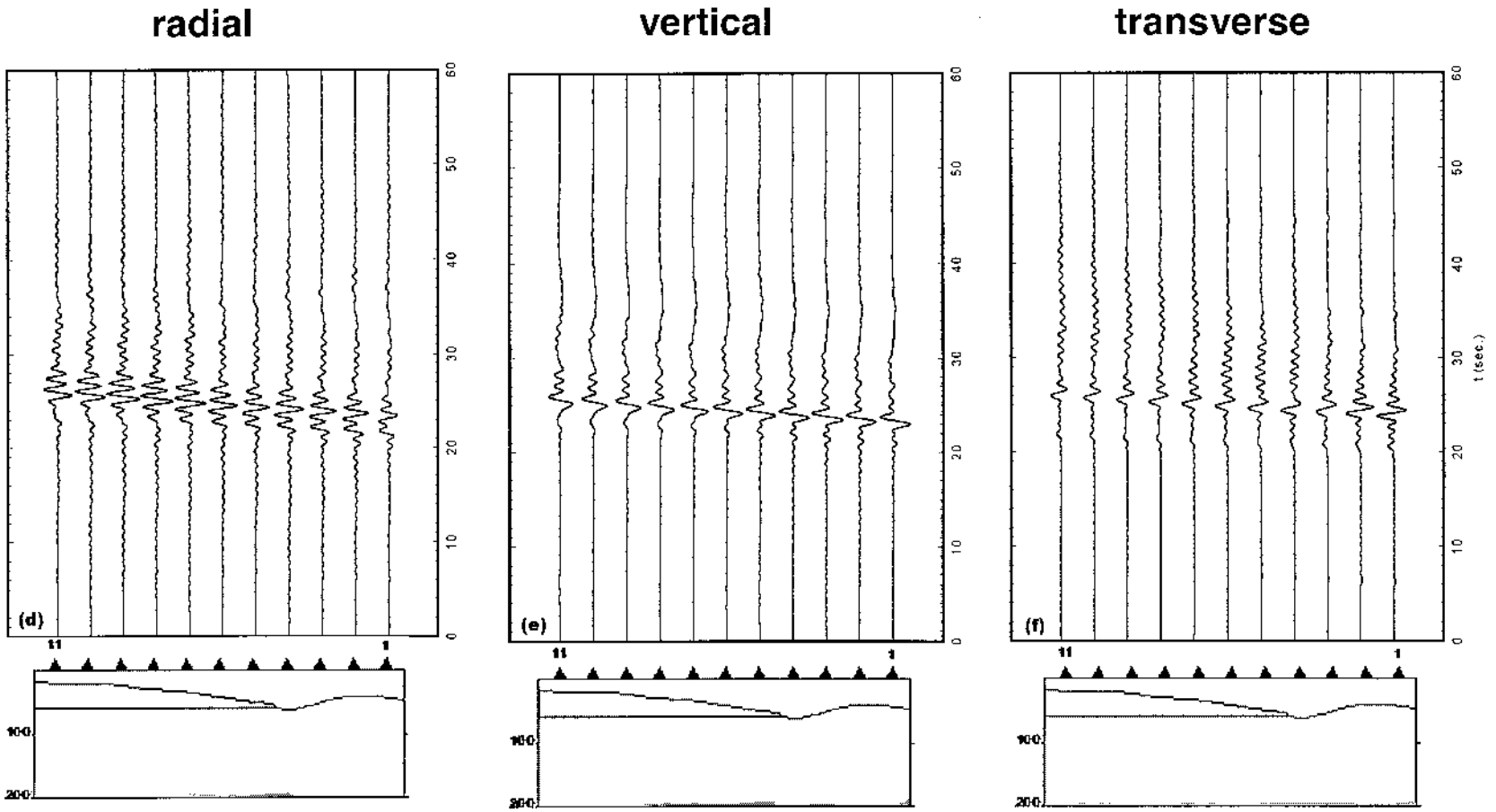


| No | Density | Vp | Vs | Qp | Qs |
|---|---|---|---|---|---|
| 1 | 1.85 | 1.8 | 0.5 | 100 | 50 |
| 2 | 2 | 1.9 | 0.6 | 200 | 100 |
| 3 | 2.3 | 2.2 | 0.8 | 400 | 200 |

1
2
3

Fig. 4 (d-f)

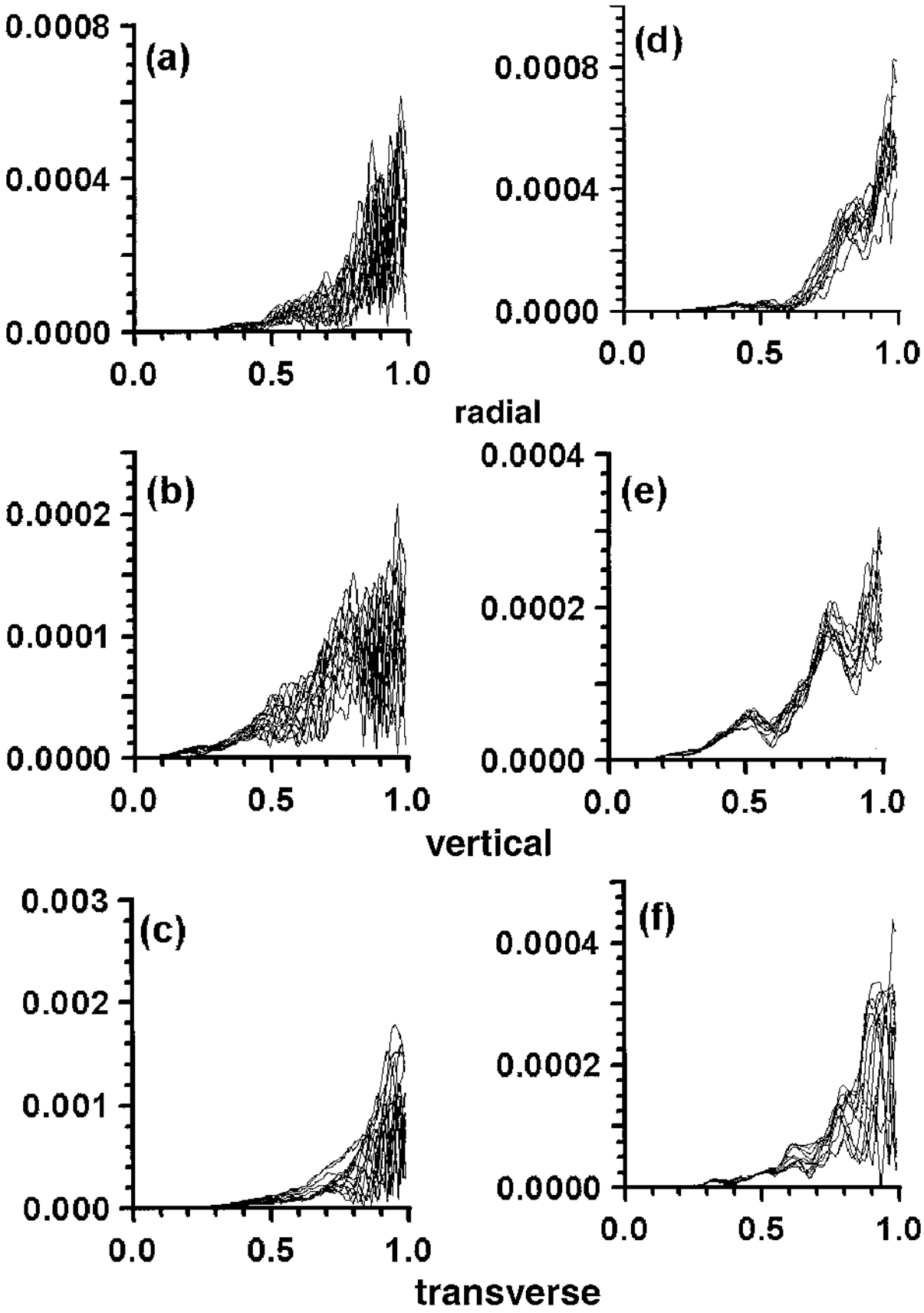
(a)
0.0008
0.0004
0.0000
0.0
0.5
1.0
(d)
0.0008
0.0004
0.0000
0.0
0.5
1.0
radial
(b)
0.0002
0.0001
0.0000
0.0
0.5
1.0
(e)
0.0004
0.0002
0.0000
0.0
0.5
1.0
vertical
(c)
0.003
0.002
0.001
0.000
0.0
0.5
1.0
(f)
0.0004
0.0002
0.0000
0.0
0.5
1.0
transverse

Fig. 5

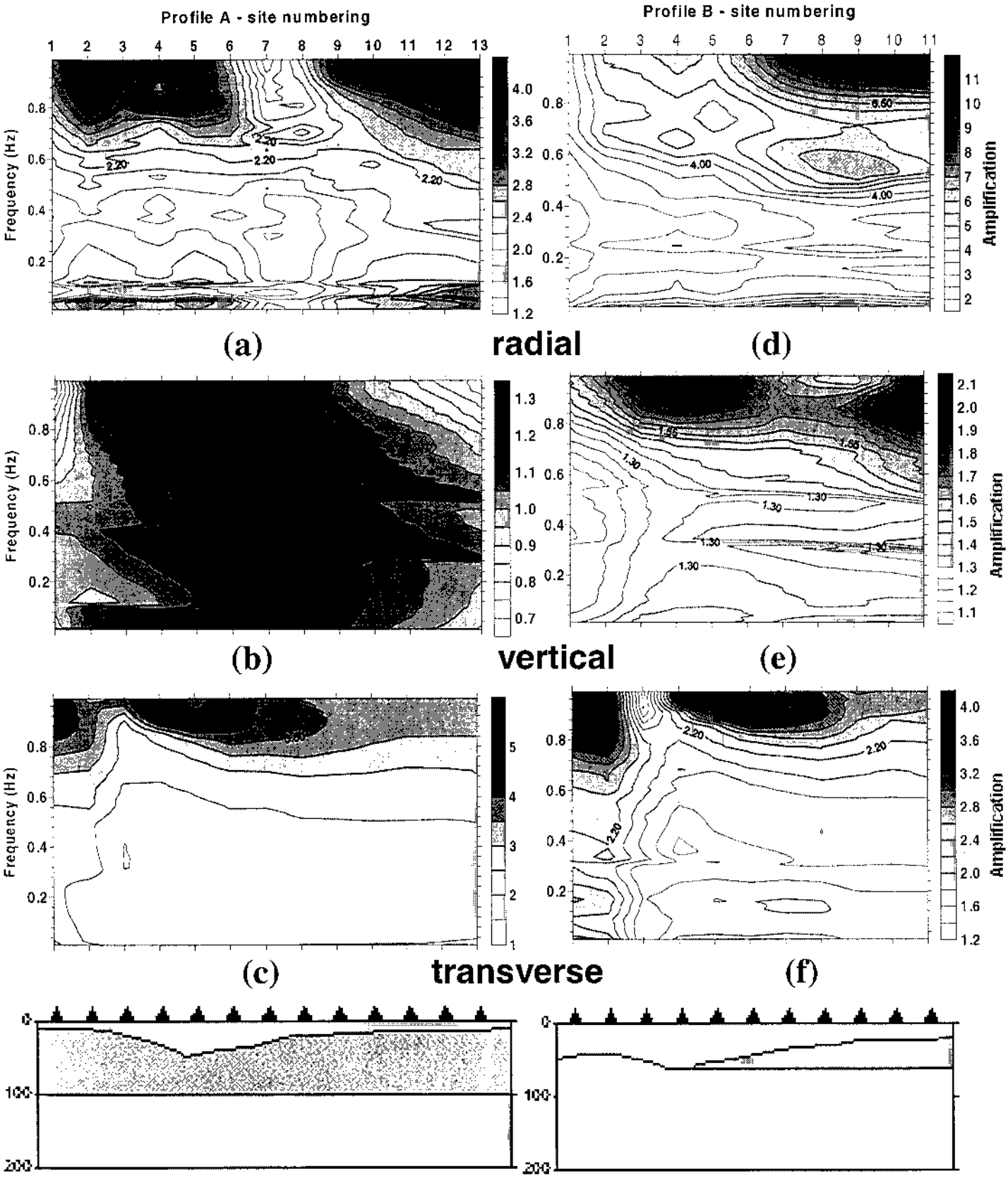
Profile A - site numbering
Profile B - site numbering
Frequency (Hz)
Amplification
(a)
radial
(d)
(b)
vertical
(e)
(c)
transverse
(f)
0
100
200

Fig. 6

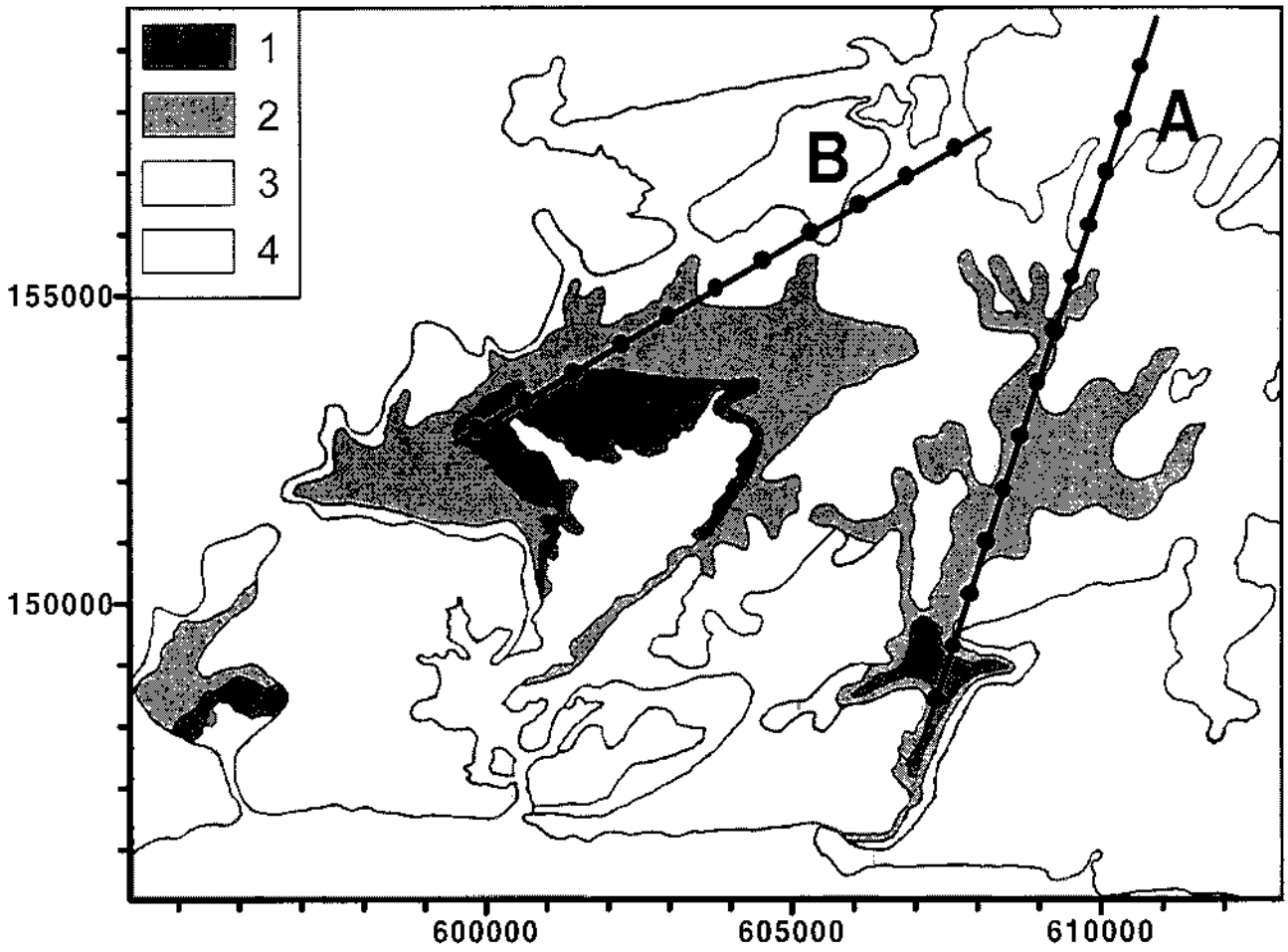


Fig. 7a

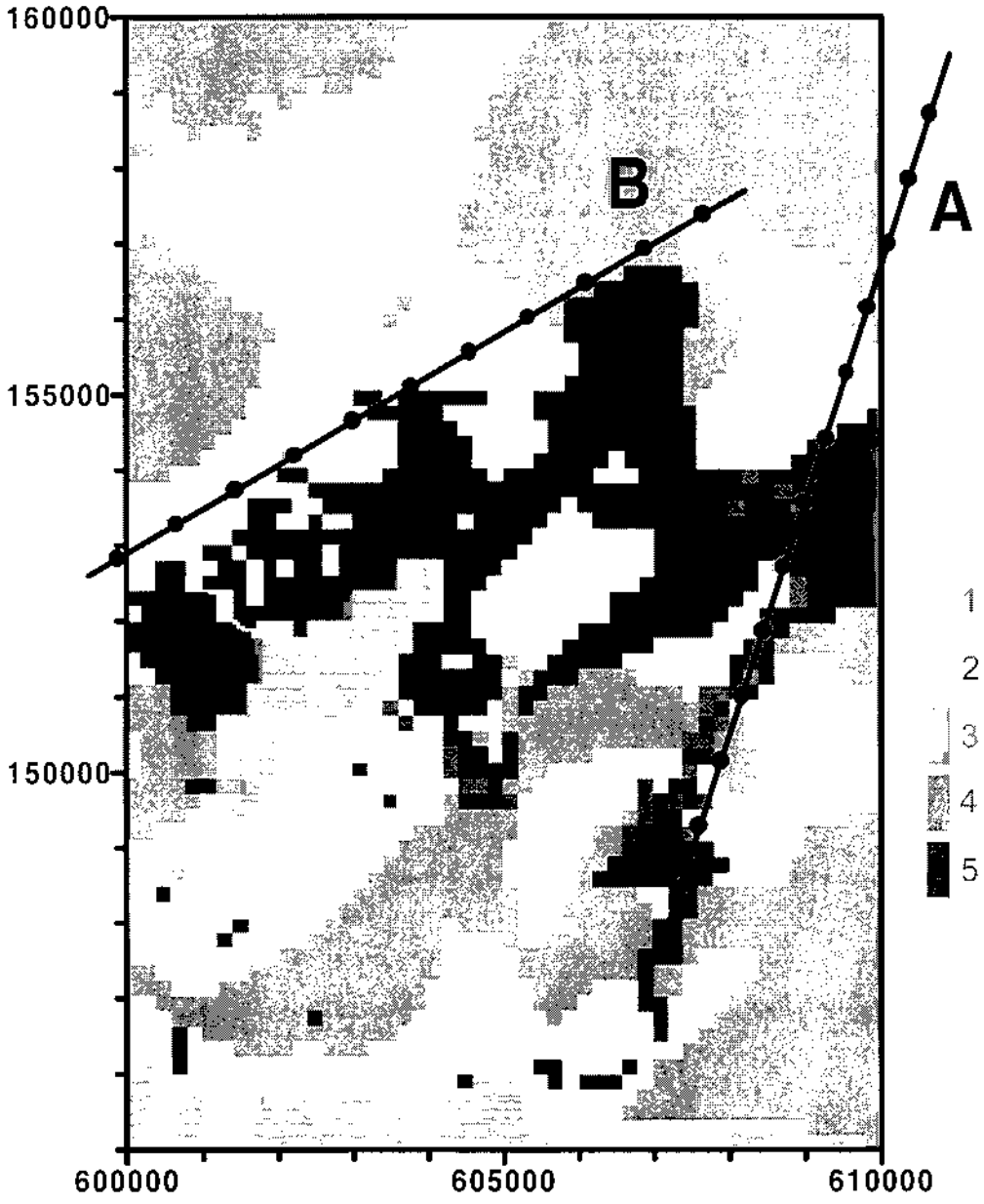


Fig. 7b